Fermi Surface of Magnesium.
IV. Magnetoresistance Study of Open Trajectories*

C. B. Friedberg† and R. W. Stark

*Department of Physics and The James Franck Institute, The University of Chicago
Chicago, Illinois 60637*
(Received 1 November 1971)

Measurements of the magnetoresistance of high-purity single crystals of magnesium were made in order to determine the magnetic field directions for which open trajectories exist on the magnesium Fermi surface. Nine distinct series of open trajectories with net directions parallel to the basal plane of reciprocal space were observed. These trajectories have basic periodicities extending up to nine Brillouin zones and result from magnetic breakdown between the monster and cigar. The magnetic field directions for which these trajectories exist are shown to be in excellent agreement with the predictions of the Fermi-surface model proposed by Kimball, Stark, and Mueller. Measurements for the open trajectory parallel to the hexagonal axis in reciprocal space are also reported; these show a clear indication of the onset of magnetic breakdown across the spin-orbit gap separating the monster and the cap.

INTRODUCTION

The original detailed investigation of the galvanomagnetic properties of magnesium[1,2] by Stark, Eck, and Gordon (henceforth referred to as SEG) demonstrated the importance of magnetic breakdown[3-5] in establishing the character of the semiclassical electron trajectories in a metal. Studies of open trajectories generated by magnetic breakdown for particular directions of $\vec{H}$ provided information about the dimensions of the magnesium Fermi surface. An equivalent investigation for zinc, whose Fermi surface and band structure are in many ways similar to those for magnesium, demonstrated in addition that the presence of Landau quantization affects the magnetic-breakdown probabilities in such a way as to be directly manifested in the galvanomagnetic properties.[6-9] The effects of quantization were not revealed in the original magnesium work because of the high concentration of impurities in the crystals (the magnesium residual resistance ratios $R_{300°K}/R_{4.2°K}$ were ~450 as compared with 5×10^4 for zinc). The possibility that studies with purer magnesium could lead to further understanding of these quantization effects provided the impetus for purification efforts[10] which resulted in single crystals of magnesium having residual resistance ratios in excess of 10^6. These crystals have been used for extensive studies of the effects of magnetic breakdown in both the semiclassical and quantum regimes. However, the work that has been reported has been limited to only the single case for which $\vec{H}$ is parallel to the sixfold axis.[5,9]

In the interval since the original studies, the Fermi-surface dimensions of magnesium have been determined both experimentally and theoretically to a high degree of precision.[11-13] These dimensions

were used to predict the directions of $\vec{H}$ which yield open trajectories; the predictions, although in qualitative agreement, were not in quantitative agreement with results of SEG. The discrepancies were believed to be associated with experimental difficulties arising from the low purity of the samples used in SEG. The investigations reported here were undertaken in an effort to eliminate this apparent inconsistency. This is the fourth paper in a series aimed explicitly at the determination of the Fermi surface and electronic band structure of magnesium. The results of the first three will be relied upon in the following discussion and will be referred to as I, II, and III (Refs. 11, 12, and 13, respectively).

The magnesium lattice is hexagonal close packed, having two atoms per unit cell, each of which contributes two electrons, giving a total of four electrons in the conduction band for each unit cell. Hence, the number of conduction electrons is exactly twice the number of available states in the first Brillouin zone of reciprocal space; in such a case the number of unfilled states in the first two Brillouin zones must be equal to the number of filled states in all higher zones. So, in the absence of interband transitions, the number of electron states n_e equals the number of hole states n_h, and magnesium is said to be compensated. From the viewpoint of conductivity theory, the concept of electrons and holes in a metal refers to the orbital dynamics of the conduction electrons in a magnetic field.[14] The "number" of such electrons (holes) is equivalent to the volume in $\vec{k}$ space which is enclosed by electron- (hole-) like orbits and in general is dependent on $\vec{H}$. The direction of $\vec{H}$ enters since for some directions orbits are generated which are not closed but are instead open; both the direction and magnitude of $\vec{H}$ are important when

magnetic breakdown is possible.

The asymptotic field dependence of high-field magnetoresistance is sensitive to the relative number of electrons and holes, and to the existence of open orbits. The results of the theory of high-field magnetoresistance developed by Lifshitz et al.[15] which are pertinent to this experiment may be summarized as follows:

(i) If for a given magnetic field direction there are no open trajectories, the magnetoresistance grows quadractically with the magnetic field strength H if the number of electrons equals the number of holes (i. e., $n_e = n_h$); the magnetoresistance saturates at a constant value if the number of electrons is unequal to the number of holes ($n_e \neq n_h$).

(ii) If open trajectories exist for a given field direction,

$$\rho = A + B H^2 \cos^2\gamma, \tag{1}$$

where ρ is the transverse magnetoresistance, γ is the angle between the current density $\vec{J}$ and the open-orbit direction in reciprocal space, and A and B are constants.

In a magnetic field, the representation of electron states as time-dependent $\vec{k}$ vectors traveling on a single sheet of the Fermi surface is only an approximation. The probability that electrons will tunnel through the small gaps separating different sheets of the Fermi surface, and, thus, traverse more nearly free-electron-like orbits, increases with larger applied magnetic field strengths.[5] This magnetic-breakdown effect can change the effective topology of the Fermi surface and, in magnesium, destroy the volume compensation. Thus, as the breakdown field is approached, the change in the Fermi-surface topology can be observed as a change in the magnetoresistance.

Since in the absence of magnetic breakdown magnesium is compensated, the magnetoresistance must be proportional to the square of the applied field for all magnetic field directions which do not permit open orbits. The magnetoresistance can saturate only when the current direction is perpendicular to an open trajectory in reciprocal space, or when magnetic breakdown occurs.

EXPERIMENTAL PROCEDURE

Single crystals of high-purity magnesium were grown directly from the vapor phase under high vacuum.[10] The rectangular samples (approximate dimensions $0.030 \times 0.030 \times 0.250$ in.) used for most of this experiment were cut from such crystals with a string saw using a 10% aqueous solution of HCl after alignment by standard x-ray techniques. The samples were cut for current directions along the crystallographic $[11\bar{2}0]$ and $[0001]$ axes. Four copper spots equally spaced along the sample length were deposited on one surface of each sample by means of dc sputtering in an argon atmosphere. To avoid inducing strain into the samples by the relative thermal contraction of the lead wires upon thermal cycling, small-diameter (0.003-in.) wires were used for both the current and potential leads. These were soldered to the copper spots using indium solder.

The sample was "glued" at one end to a demountable epoxy holder with a small drop of Dow-Corning 200 (silicone) fluid of viscosity 2.5 $\times 10^6$ cP at 25° C. This "glue" retains sufficient fluidity so that the sample can contract relative to the holder upon cooling but at the same time is viscous enough at low temperatures to prevent the sample from moving in the high magnetic field when current is introduced.

After the orientation of the sample was refined by further x-ray alignment, the sample and epoxy mount were then inserted into a rotating holder such that a particular crystal axis perpendicular to the sample length was parallel to the rotation axis of the holder. This permitted the current axis of the sample to be rotated ± 90° with respect to the vertical by means of a gear train linking a forty-turn dial outside the liquid-helium Dewar to the sample holder inside. Data were taken for a given tilt angle by continuously recording the output voltage across the potential leads as the magnet was rotated through 180° in the horizontal plane. Utilization of these two perpendicular rotation axes allowed magnetoresistance measurements for arbitrary field directions relative to the current direction rather than limited measurements for a single plane of field directions. Final orientation of the sample relative to $\vec{H}$ was achieved by tilting the entire cryostat up to 4° about a third rotation axis perpendicular to the other two.

Calibration of the angle settings on the rotating holder was obtained directly from the symmetry of the data. The absolute calibration was accurate to one part in 10^3. Relative reproducibility and linearity of the angle adjustments was better than 1 min of arc.

Measurements were taken at temperatures between 1.2 and 4.2 °K in magnetic fields up to 25 kG, with typical currents of 0.6–2.25 A applied to the specimen. The usual procedure was to take a series of "rotation diagrams" (that is, plots of magnetoresistance vs magnetic field direction for a given magnetic field strength, as in Fig. 1) for successive orientations of the sample current direction. In general, the current axis was rotated in steps of approximately 3° from vertical to horizontal. The sample was then removed from the cryostat and rotated 90° about its current axis with respect to the axis of rotation of the holder and the same data taking procedure was repeated. In this way, the 4π solid angle of possible magnetic
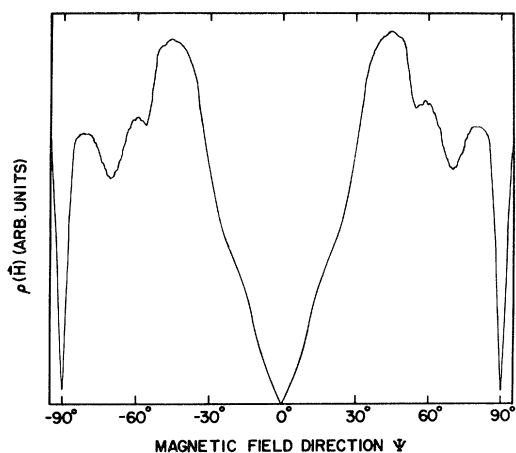
FIG. 1. Transverse-magnetoresistance rotation diagram of a pure single crystal of magnesium for which $\vec{J}$ is parallel to $[11\bar{2}0]$. $\vec{H}$ is parallel to $[0001]$ at $\Psi = 0°$ and is parallel to a $[10\bar{1}0]$-type axis at $\Psi = \pm 90°$. The magnetic field strength is 25 kG.

field directions was covered by a mesh of experimental data for each sample. In regions of rapidly changing features on the rotation diagrams, rotation curves were taken at intervals as small as 0.1°, giving a much finer grid of data. The directions of $\vec{H}$ for which the magnetoresistance indicated special features were further investigated by plotting the magnetoresistance as a function of magnetic field strength.

EXPERIMENTAL RESULTS

A typical magnetoresistance rotation diagram is shown in Fig. 1. This particular curve is for a sample in which $\vec{J}$ was along $[11\bar{2}0]$ and for which the plane of rotation of $\vec{H}$ was perpendicular to $\vec{J}$ (the case of transverse magnetoresistance). The sharp spikelike minima at $\Psi = \pm 90°$, where $\vec{H}$ crosses the basal plane, is the residual manifestation of an open trajectory. In this case, the direction of the open trajectory is along the sixfold axis of reciprocal space. This rotation curve may be compared directly with those in Fig. 7 of SEG which were taken at 18 and 61.5 kG with a sample having a resistivity ratio of 450. The distinct features visible in our curve at a modest field strength (25 kG) result from the high purity and absence of strain in these new samples.

As the plane of the magnetic field is tilted about the $[10\bar{1}0]$-type axis (at $\Psi = \pm 90°$ in Fig. 1) with respect to $\vec{J}$, other sharp spikes appear in the rotation diagram near $\Psi = 0°$. A segment about $\Psi = 0°$ of a rotation diagram taken for a tilt angle of 8.6° is shown in Fig. 2. The broad minimum at $\Psi = 0°$ is the persistence of the broad minimum in Fig. 1; the four pairs of sharp minima on either side of $\Psi = 0°$ result from open trajectories directed per-

pendicular to the sixfold axis of $\vec{k}$ space. One normally presents a compendium of all directions of $\vec{H}$ resulting in open trajectories in a stereographic projection. The eight sharp minima in Fig. 2 become eight points on such a projection; the loci of these points as the tilt angle is varied define the directions of $\vec{H}$ associated with a particular open trajectory.

Figures 3(a) and 3(b) show the stereographic projection of all those directions of $\vec{H}$ in reciprocal space which were found to generate open trajectories in this experiment. Directions of $\vec{H}$ are given by the coordinates θ, the polar angle measured from $\vec{b}_1$ (parallel to the real space $[0001]$ axis), and φ, the azimuthal angle in the basal plane measured from $\vec{b}_2$. $\vec{b}_1$, $\vec{b}_2$, and $\vec{b}_3$ are the basis vectors of the reciprocal-space lattice as described in I. The stereogram [Fig. 3(a)] shows only those regions of open trajectories which were reported previously (Fig. 3 of SEG). The circular region about the pole of the stereogram, for which $\vec{H}$ is within ~ 4.5° of $\vec{b}_1$, is a two-dimensional region having open trajectories with net directions parallel to the basal plane. The radial lines are one-dimensional regions with open trajectory directions perpendicular to the plane represented by the corresponding radial line. The periphery of the stereogram is also a one-dimensional region representing trajectories parallel to $\vec{b}_1$.

In addition, many new regions of open trajectories were observed. These are shown in Fig. 3(b), which is an enlargement of a central slice ($-30°$ $\leqslant \varphi \leqslant 30°$, $\theta \leqslant 15°$) of Fig. 3(a). Parts of the long and short radial lines of Fig. 3(a) are shown, as well as seven other distinct types of one-dimensional regions of open trajectories. These new radial lines also represent orbits with net directions parallel to the basal plane. All of the directions of $\vec{H}$ for which our data indicated open tra-
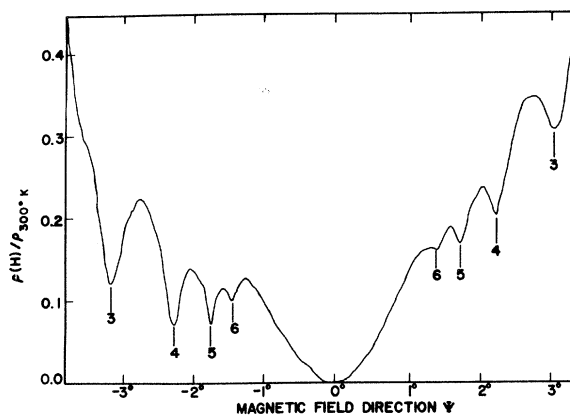
FIG. 2. A segment of a magnetoresistance rotation diagram taken at 23 kG. The sharp minima labeled 3–6 result from the presence of open trajectories.
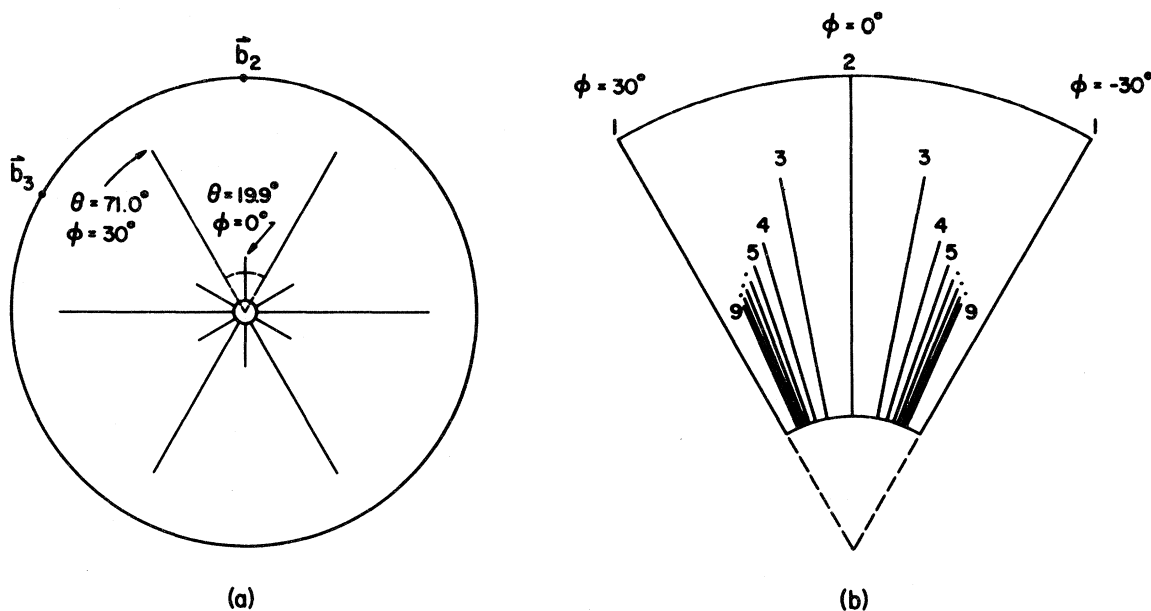
FIG. 3. Sterographic projections of all of the directions of $\vec{H}$ giving rise to open trajectories in magnesium. The basis vectors ($\vec{b}_1$, $\vec{b}_2$, $\vec{b}_3$) of the reciprocal-space lattice are indicated. $\vec{b}_1$ is parallel to the pole of the stereogram. (a) Those open trajectory regions originally reported in SEG. The small pie-shaped region inset is shown expanded to the right. (b) Open trajectory regions which were not reported by SEG, labelled 3–9.

jectories are included in a superposition of both stereograms.

The quantitative information needed to make comparison to Fermi-surface models is the exact angular range of $\vec{H}$ for which each open trajectory exists. This means that one must measure the "length" of each radial line (the angle $\theta_c^{(n)}$ at which the nth open trajectory cuts off) as well as the corresponding $\varphi^{(n)}$. This can be done with high accuracy. For example, the length of the long radial lines (at $\varphi^{(1)} = 30°$) is measured by taking successive rotations of $\vec{H}$ through the end of the line for various tilt angles of $\vec{J}$ from the vertical. Figure 4(a) shows segments of a series of such rotation curves near the end of this line for a sample having $\vec{J}$ parallel to [0001]. The presence of a small but sharp spike at $\Psi = 0°$ in any of these curves shows that the radial line persists to that angle. The spike cuts off very sharply as the tilt angle increases. In fact, from Fig. 4(b), which shows a portion of this same data with increased gain and a finer spacing of tilt angles, one can clearly see that the open trajectory spike vanishes within 0.1°. Although in terms of the external angle readings of the rotating holder, these data were consistently reproducible, the absolute length of the radial lines were not determined to this great an accuracy because of an uncertainty of about 0.25° in the absolute alignment of the crystal axes. Including this uncertainty, we find for the long radial lines $\theta_c^{(1)} = 71.0° \pm 0.25°$, whereas the value re-

ported in SEG was only $\theta_c^{(1)} \simeq 60°$. A similar measurement on a sample with $\vec{J}$ parallel to [11$\bar{2}$0] gave $\theta_c^{(1)} = 70.9° \pm 0.25°$.

The length of the short radial lines of Fig. 3(a) was measured by the same technique. In this case, the best data are obtained with $\vec{J}$ parallel to [0001] rather than [11$\bar{2}$0]. This is because the factor $\cos^2 \gamma$ in Eq. (1), which multiplies the nonsaturating term in the high-field magnetoresistance for these open trajectories, vanishes for $\vec{J}$ parallel to [0001] but not for $\vec{J}$ parallel to [11$\bar{2}$0]. The lengths of four equivalent short radial lines were measured. These measurements give $\theta_c^{(2)} = 19.9° \pm 0.25°$. The value reported in SEG was $\theta_c^{(2)} \simeq 15°$. The fact that both $\theta_c^{(1)}$ and $\theta_c^{(2)}$ as determined in this experiment are greater than the corresponding values obtained by SEG results from the significant improvement in the purity of the samples used here.

The lengths of the seven shorter sets of radial lines of Fig. 3(a) were measured similarly. For $n \leq 7$, each of these lines was also observed to cut off within 0.1°. For $n = 8$ and $n = 9$, the cutoff was not as definitive. The uncertainty of $\theta_c^{(n)}$ for $n \leq 7$ is $\pm 0.25°$. For $n > 7$, the uncertainty is $\pm 0.5°$ as a result of the less distinct cutoffs. The lengths of all the radial lines, as measured by this method, are tabulated in Table I.

Measurements of the dimensions of the central two-dimensional region of the stereogram were not as definitive in establishing limiting angles as was possible for the one-dimensional radial line regions.
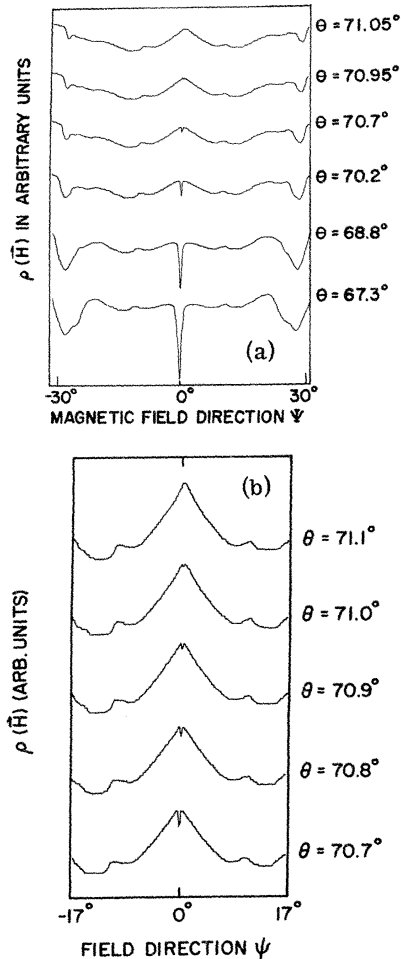
FIG. 4. Portions of magnetoresistance rotation diagrams for $\vec{J}$ parallel to [0001] and $\vec{H}$ near the end of one of the long radial lines ($n=1$) shown in Fig. 3(a). The sharp spike occurs as $\vec{H}$ sweeps across the radial line. Ψ measures the angle of $\vec{H}$ from the plane containing the radial line. θ measures the angle in this plane between $\vec{H}$ and $\vec{b}_1$. (a) Rotation diagrams taken over a range within $4°$ of the end of the radial line. (b) Expanded plots of the rotation diagrams near the sharp spike for successive increments of $0.1°$ in θ. The spike is barely evident at $71.0°$ but has completely disappeared at $71.1°$.

Our best data show that $\theta \leq 4.5° \pm 0.5°$. One should note that a general characteristic of an open trajectory generated in this two-dimensional region is that the trajectory is aperiodic with respect to the reciprocal lattice, that is, its net direction of propagation is not generally along an axis of crystal symmetry.

The propagation direction of any of the open trajectories associated with the radial lines, on the other hand, is directly along an axis of symmetry in reciprocal space. For example, let us consider only those radial lines occurring in the pie-shaped segment of the stereogram defined by the range of

azimuthal angle $270° \leq \varphi \leq 300°$. The ($n=1$)-type radial line ($\varphi = 270°$) has an open trajectory in $\vec{k}$ space along $\vec{b}_2$, while the ($n=2$)-type radial line ($\varphi = 300°$) has an open trajectory in the direction $\vec{b}_2 + \vec{b}_3$. In general, for $n \geq 2$, the nth-type radial line has an open trajectory in the direction $(n-1)\vec{b}_2 + \vec{b}_3$. The value of $\varphi^{(n)}$ calculated for each of these symmetry directions is listed in Table I. Compared with these are the values of $\varphi^{(n)}$ observed for the radial lines in our experiment; the discrepancy between the predicted and measured values of $\varphi^{(n)}$ is no larger than $0.3°$ until $n \geq 7$. Although this series undoubtedly persists to very large n, the close angular spacing of the successive minima in the magnetoresistance rotation diagrams prohibits their accurate resolution beyond $n = 9$, and is the source of the discrepancy for $n = 8$ and $n = 9$.

CONSISTENCY BETWEEN EXPERIMENT AND THEORY

The results of the nonlocal orthogonalize-plane-wave (OPW) pseudopotential calculations reported in III showed that the magnesium Fermi surface is only slightly perturbed from the single-OPW-model Fermi surface shown in Fig. 3 of I. The perturbations consist primarily of a rounding and smoothing of some of the sharp edges exhibited by the OPW model. The results of III show also that the energy gaps between the monster and the cigar and between the monster and the cap are all small enough to allow a significant amount of magnetic breakdown in fields as low as 1 kG. In general, the results of III agree well with the qualitative requirements of the interpretation proposed by SEG for the origin of the two-dimensional region of open trajectories around $\vec{b}_1$ and for the two longest set of open trajectory radial lines that emanate from the two-dimensional region. The SEG interpretation required interband tunneling from the monster to the cigar via magnetic breakdown; the limiting directions of $\vec{H}$ which yielded these open trajectories were related in that interpretation to certain limiting geometric features on the monster and to a possible limitation in height of the region for which the band gap between the monster and the cigar is small enough to permit a significant degree of magnetic breakdown. It was shown in III, however, that the energy gap between the monster and the cigar is small and relatively constant along the entire length of the cigar; Fig. 7 of III graphically demonstrates that the cigar and monster are essentially degenerate in the ΓKHA plane of the Brillouin zone. All limitations upon the range of $\vec{H}$ for any of these open trajectories must hence result solely from geometric limitations on the monster.

The nonlocal OPW pseudopotential results of III have recently been used to generate a dense array of electron wave vectors $\vec{k}$ for the magnesium Fermi surface.[16] These points satisfy the energy re-

lation $\vec{k}(E) = \vec{k}(E_F)$, where E_F is the Fermi energy; also tabulated for each $\vec{k}$ point is the local value of the Fermi veloctiy $\vec{V}_F(E_F)$. The density is such that each point in the array represents less than 10^{-5} of the surface area of the single-OPW sphere. Thus this entire array yields an excellent geometric representation of the magnesium Fermi surface from which it is then relatively easy to determine the theoretical limiting angles $\theta_c^{(n)}$ for each of the radial lines on the stereogram in Figs. 3(a) and 3(b).

This is done by first generating computer projections of the portion of the array for the monster in the repeated-zone scheme onto planes perpendicular to the appropriate open trajectory symmetry directions listed in Table I. A plane perpendicular to $\vec{H}$ which contains an open trajectory is represented by a straight line in such a projection. Assuming that magnetic breakdown is equally probable along the entire length of the cigar as indicated in III, one may thus readily determine the geometrical features which limit a given open trajectory. As a general result, we find that for $n \geq 2$, the essential feature responsible for limiting the open trajectories is the horizontal waist of the monster. For $n = 1$, the open trajectory is limited by both the horizontal waist and the diagonal arms of the monster. All of the theoretical predictions for the limiting polar angles $\theta_c^{(n)}$ are listed in Table I, where they are compared with the experimental values. The excellent agreement between theory and experiment provides further verification for the accuracy of the nonlocal OPW pseudopotential formulation reported in III.

OPEN TRAJECTORY PARALLEL TO $\vec{b}_1$

For all directions of $\vec{H}$ parallel to the basal plane [denoted by the periphery of the stereogram in Fig. 3(a)], an open trajectory is generated parallel to $\vec{b}_1$. This trajectory traverses the diagonal arms of the monster[17] and results when spin-orbit interactions remove the crystal field degeneracies between the cap and monster in the AHL plane of the Brillouin zone.[18] The energy gap that is induced is sufficiently small that magnetic breakdown is expected to be of importance for magnetic fields as small as 1 kG. The details of this orbit are fully discussed in Ref. 17 and shown there in Fig. 1. The only direct experimental evidence for this open trajectory which has previously been reported is the magnetoacoustic resonance result in Ref. 17. No evidence of this low-field trajectory was reported by SEG.

Figure 5 shows the transverse magnetoresistance vs magnetic field strength of a magnesium crystal for which $\vec{J}$ is parallel to $[11\bar{2}0]$ and $\vec{H}$ is parallel to a $[10\bar{1}0]$-type axis. In this case $\vec{J}$ is perpendicular to the open trajectory direction in $\vec{k}$ space, so that the magnetoresistance is expected to saturate. The experimental data show saturation for $|H| \lesssim 600$ G. However, for $|H| \gtrsim 600$ G the magnetoresistance ceases to saturate and increases with increasing H. This behavior results from the onset of magnetic breakdown across the spin-orbit-induced gap in the AHL plane. The magnetic field strength for which the deviation from saturation occurs is strikingly similar to that reported in Ref. 17 for the loss in amplitude with magnetic field strength

TABLE I. Summary of experimental and theoretical information on open trajectories directed parallel to the $\vec{b}_2 - \vec{b}_3$ plane.

Open trajectory	Symmetry direction	Direction of trajectory in the basal plane measured from $\vec{b}_2$		Critical angle (length of radial line)	
		$\varphi^{(n)}$ Predicted (deg)	$\varphi^{(n)}$ Measured (deg)	$\theta_c^{(n)}$ Predicted (deg)	$\theta_c^{(n)}$ Measured (deg)
$n = 1$ (long radial line)	$\vec{b}_2$	0.0	0.0	71.0	71.0
$n = 2$ (short radial line)	$\vec{b}_2 + \vec{b}_3$	30.0	30.0	20.0	19.9
$n = 3$	$2\vec{b}_2 + \vec{b}_3$	19.1	18.9	12.0	11.8
$n = 4$	$3\vec{b}_2 + \vec{b}_3$	13.9	14.2	10.2	10.0
$n = 5$	$4\vec{b}_2 + \vec{b}_3$	10.9	10.9	9.5	9.3
$n = 6$	$5\vec{b}_2 + \vec{b}$	8.9	8.6	9.1	8.6
$n = 7$	$6\vec{b}_2 + \vec{b}_3$	7.6	7.0	8.9	8.3
$n = 8$	$7\vec{b}_2 + \vec{b}_3$	6.6	5.7	8.7	8.1
$n = 9$	$8\vec{b}_2 + \vec{b}_3$	5.8	4.4	8.5	7.9
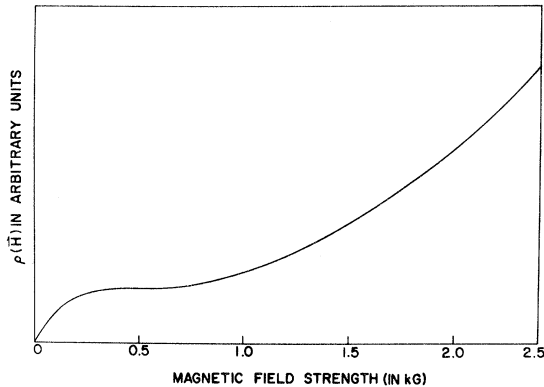
FIG. 5. Transverse magnetoresistance vs magnetic field strength for $\vec{J}$ parallel to [11$\bar{2}$0] and $\vec{H}$ parallel to a [10$\bar{1}$0]-type axis. The saturation for $H \leq 600$ G results from the open trajectory parallel to $\vec{b}_1$. The deviation from saturation for $H \geq 600$ G results from the gradual loss of the open trajectory due to magnetic breakdown.

of the magnetoacoustic open-orbit resonance.

Falicov and Sievert[19] performed, as a function of the magnetic-breakdown probability $P = e^{-H_0/H}$, model calculations of the magnetoresistive behavior for an open trajectory system similar to that which exists in magnesium. H_0 is the critical magnetic field strength for magnetic breakdown which characterizes a particular interband transition. Their theoretical results which describe an open trajectory situation like that for magnesium are shown in Fig. 5 of their paper.[19] The pertinent result is that the deviation of the magnetoresistance from saturation occurs at a field strength of about $H_0^{FS}/5$, where the superscript FS indicates an implicit dependence on their theory for the magnetoresistance. Thus, since the deviation shown in our data in Fig. 5 occurs at about 600 G, we conclude that for the spin-orbit gap across the

AHL plane between the monster and the cap, H_0^{FS} = 3 kG. The value of H_0 calculated in Ref. 17 using some of the structure information of III together with the geometry and velocities appropriate for the single-OPW model is H_0 = 900 G. More recent calculations show that in the vicinity of the AHL plane the band velocity from III is actually somewhat smaller than that from the single-OPW model yielding a value of H_0 based solely on III that is in good agreement with the value H_0^{FS} = 3 kG.

The data for the dependence of the transverse magnetoresistance on magnetic field strength for $|\vec{H}| \geq 2500$ G is complicated by quantum interference effects and has been treated in detail elsewhere.[20]

CONCLUSIONS

New magnetoresistance measurements of the directions of $\vec{H}$, which generate open trajectories on the Fermi surface of magnesium, agree well with the predictions of the nonlocal OPW pseudopotential of III. This provides further experimental confirmation for the accuracy of that pseudopotential. The earlier results of SEG, though qualitatively correct, are not quantitatively correct because of the relatively low purity of the crytals used in their experiment.

These new measurements also show, for the first time, direct evidence in the magnetoresistance for the onset of magnetic breakdown on the open trajectory directed along the hexagonal axis of reciprocal space. The value of H_0^{FS} = 3 kG obtained from these data by applying the results of Falicov and Sievert agrees well with that obtained solely from the band-structure information in III.

ACKNOWLEDGMENTS

*Supported in part by NSF, ARO (Durham), and ARPA.

†Fannie and John Hertz Foundation Predoctoral Fellow.

[1] R. W. Stark, T. G. Eck, W. L. Gordon, and F. Moazed, Phys. Rev. Letters 8, 360 (1962).

[2] R. W. Stark, T. G. Eck, and W. L. Gordon, Phys. Rev. 133, A443 (1964).

[3] M. H. Cohen and L. M. Falicov, Phys. Rev. Letters 7, 231 (1961).

[4] E. I. Blount, Phys. Rev. 126, 1636 (1962).

[5] R. W. Stark and L. M. Falicov, in Progress in Low Temperature Physics, edited by C. J. Gorter (North-Holland, Amsterdam, 1967), Vol. V.

[6] R. W. Stark, Phys. Rev. Letters 9, 482 (1962).

[7] R. W. Stark, Phys. Rev. 135, A1698 (1964).

[8] A. B. Pippard, Phil. Trans. Roy. Soc. London A256, 317 (1964).

[9] L. M. Falicov, A. B. Pippard, and P. R. Sievert, Phys. Rev. 151, 498 (1966).

[10] R. W. Stark (unpublished).

[11] J. B. Ketterson and R. W. Stark, Phys. Rev. 156,

748 (1967).

[12] R. W. Stark, Phys. Rev. 162, 589 (1967).

[13] J. C. Kimball, R. W. Stark, and F. M. Mueller, Phys. Rev. 162, 600 (1967).

[14] R. G. Chambers, Proc. Roy. Soc. (London) A65, 458 (1952).

[15] I. M. Lifshitz, M. I. Azbel, and M. I. Kaganov, Zh. Eksperim. i Teor. Fiz. 31, 63 (1956) [Sov. Phys. JETP 4, 41 (1957)]; and I. M. Lifshitz and V. G. Peschanskii, ibid. 35, 1251 (1958) [8, 875 (1959).

[16] P. Roach, Phys. Rev. B 4, 1748 (1971).

[17] R. V. Kollarits, J. Trivisonno, and R. W. Stark, Phys. Rev. B 2, 1508 (1970).

[18] L. M. Falicov and M. H. Cohen, Phys. Rev. 130, 92 (1963).

[19] L. M. Falicov and P. R. Sievert, Phys. Rev. 138, A88 (1965).

[20] R. W. Stark and C. B. Friedberg, Phys. Rev. Letters, 26, 556 (1971); and unpublished.